The effect of pitch in multislice spiral/helical CT

Ge Wang[a] and Michael W. Vannier
Department of Radiology, University of Iowa, Iowa City, Iowa 52242

(Received 20 November 1998; accepted for publication 30 September 1999)

The purpose of this study is to understand the effect of pitch on raw data interpolation in multislice spiral/helical computed tomography (CT) and provide guidelines for scanner design and protocol optimization. Multislice spiral CT is mainly characterized by the three parameters: the number of detector arrays, the detector collimation, and the table increment per x-ray source rotation. The pitch in multislice spiral CT is defined as the ratio of the table increment over the detector collimation in this study. In parallel to the current framework for studying longitudinal image resolution, the central fan-beam rays of direct and opposite directions are considered, assuming a narrow cone-beam angle. Generally speaking, sampling in the Radon domain by the direct and opposite central rays is nonuniform along the longitudinal axis. Using a recently developed methodology for quantifying the sensitivity of signal reconstruction from nonuniformly sampled finite points, the effect of pitch on raw data interpolation is analyzed in multislice spiral CT. Unlike single-slice spiral CT, in which image quality decreases monotonically as the pitch increases, the sensitivity of raw data interpolation in multislice spiral CT increases in an alternating way as the pitch increases, suggesting that image quality does not decrease monotonically in this case. The most favorable pitch can be found from the sensitivity-pitch plot for any given set of multislice spiral CT parameters. An example for four-slice spiral CT is provided. The study on the effect of pitch using the sensitivity analysis approach reveals the fundamental characteristics of raw data interpolation in multislice spiral CT, and gives insights into interaction between pitch and image quality. These results may be valuable for design of multislice spiral CT scanners and imaging protocol optimization in clinical applications.
[S0094-2405(99)02312-3]

I. INTRODUCTION

Recently, spiral/helical computed tomography (CT) began a transition from fan-beam to cone-beam geometry with the introduction of multislice systems.[1–6] These narrow-angle cone-beam spiral CT scanners, also referred to as multislice or multirow detector scanners, are now commercially available. Cone-beam spiral CT uses a two-dimensional (2D) detector array, allows larger scanning range in shorter time with higher longitudinal image resolution, and has important medical and other applications.[1,2,7]

In multislice spiral CT, specification of multiple acquisition and reconstruction parameters is required. For the purpose of imaging protocol optimization, the most important parameters are the number of detector arrays/rows, the detector collimation, and the table increment per x-ray source rotation. The pitch in multislice spiral CT is defined as the ratio of the table increment over the detector collimation in this study, as suggested in Refs. 6 and 8. In the above definition, without loss of generality we assume that the detector collimation for each of N detector arrays is the same, excluding the cases of either different collimation or combined ''measurement row.''

In single-slice spiral CT, the effect of pitch on image quality was studied experimentally[9–13] and theoretically.[14,15] In this report, we analyze the effect of pitch on raw data interpolation in multislice spiral CT. In the next section, a recently developed methodology for evaluating signal reconstruction from finite nonuniform samples is reviewed, and adapted for the sensitivity analysis of raw data interpolation in multislice spiral CT. In the third section, the effect of pitch is numerically studied under the assumption of four-slice spiral CT. Representative results on the sensitivity of data interpolation in multislice spiral CT are presented with respect to the pitch. In the last section, relevant issues and further research topics are discussed.

II. METHODS

A. Sensitivity analysis theory and technique

Recently, Tarczynski proposed a methodology for pointwise quality evaluation of signal reconstruction from finitely many and nonuniformly distributed samples.[16] He was inspired by the fact that reconstruction errors are generally smaller in the neighborhood of the sampling instants and increase at points remote from the samples.

A band-limited signal $f(z)$ is assumed in Ref. 16, which is expressed as

$$f(z)=\sum_{k=-\infty}^{\infty} c(k)\frac{\sin\left[\frac{\pi(z-k\Delta)}{\Delta}\right]}{\frac{\pi(z-k\Delta)}{\Delta}} = \sum_{k=-\infty}^{\infty} c(k)\,\mathrm{sinc}\left(\frac{z-k\Delta}{\Delta}\right). \quad (1)$$

where $c(k)$ are coefficients [in the case of infinite expansion terms, $c(k)=f(\Delta k)$]. Δ is the length of sampling step that meets the Nyquist criterion, $\mathrm{sinc}(z)=\sin(\pi z)/\pi z$, which is the interpolation kernel. For the sake of numerical implementation, the infinite summation is truncated as follows:

$$f(z)=\sum_{k=-M}^{M} c(k)\,\mathrm{sinc}\left(\frac{z-k\Delta}{\Delta}\right). \tag{2}$$

where M must be so selected that the interval on which $f(z)$ is of interest is deeply contained in $[-M,M]$, meaning that when k is close to either $-M$ or M, values of $c(k)$ do not contribute significantly to signal reconstruction on the interval of interest.

Suppose $f(z)$ is sampled on the set $S=\{z_1,z_2,\ldots,z_L\}$, the signal reconstruction problem is to solve the following linear equation system for $c(k)$, $k=-M,-M+1,...,-2,-1,0,1,2,...,M-1,M$,

$$f[z(i)]=\sum_{k=-M}^{M} c(k)\,\mathrm{sinc}\left[\frac{z(i)-k\Delta}{\Delta}\right]. \tag{3}$$

which can be expressed in the matrix form

$$\mathbf{A}_{L\times(2M+1)}\mathbf{X}_{(2M+1)\times 1}=\mathbf{F}_{L\times 1}, \tag{4}$$

where the unknown vector $\mathbf{X}=x(j)=c(j-M-1)$, the sample vector $\mathbf{F}=f[z(i)]$, and the matrix $\mathbf{A}$ is defined as

$$a(i,j)=\mathrm{sinc}\left[\frac{z(i)-(j-M-1)\Delta}{\Delta}\right],$$

$i=1,2,...,L$, $j=1,2,...,2M+1$.

The sensitivity function $Q(z)$ for reconstruction of $f(z)$ from $f[z(i)]$, $z_i\in S$, is calculated as follows:

$$Q(z)=\sqrt{\mathbf{G}'(z)\mathbf{B}\mathbf{B}'\mathbf{G}(z)}, \tag{5}$$

where $\mathbf{B}$ is the null space of $\mathbf{A}$, which can be found through singular value decomposition, and $\mathbf{G}'(z)=(\mathrm{sinc}((z-M\Delta)/\Delta),\ldots,\mathrm{sinc}((z+M\Delta)/\Delta))$. Generally, the rank of $\mathbf{A}$ is L (sampling locations are all different), hence in this case the dimensionality of $\mathbf{B}$ must be $2M-L+1$.

The difference must be recognized between the sensitivity in the sensitivity of signal reconstruction and that in the slice sensitivity profile. In the signal processing literature, sensitivity analysis is to determine how much influence or control various inputs or factors have over some output or process. In our study, the sensitivity analysis method is used to quantify variation in signal reconstruction given a sampling condition. On the other hand, the slice sensitivity profile is the longitudinal profile of the point spread function of a CT system.[17] A figure of merit of the slice sensitivity profile is often convenient to describe the thickness of a tomographic transaxial image, or equivalently the resolution in the table motion direction. The sensitivity of signal reconstruction is a fundamental property inherent in a data acquisition scheme, while the slice sensitivity profile is an end point of an imaging system.

The meaning of $Q(z)$ is the gain between the sup norm of the reconstructed homogeneous component of $f(z)$ and the l_2 norm of the homogeneous solution of Eq. (3). Since any solution to the linear equation system can be expressed as the sum of a particular solution and a homogeneous solution,[18] the homogeneous solution can be viewed as ''interference'' to signal reconstruction. If $Q(z_0)=0$, all reconstructions of $f(z)$ are identical at z_0. On the other hand, a large $Q(z)$ would cause a significant interference to reconstruction of $f(z)$. Recently, in order to include noise in the sampling process. Wang and Han extended Tarczynski's theory, established the minimum error bound of signal reconstruction, and demonstrated that $Q(z)$ still plays a governing role in the generalized formulation.[19]

B. Sensitivity of multislice scanning

In parallel to the current framework for studying longitudinal image resolution,[8,17,20,21] only the central fan-beam rays of direct and opposite directions are considered, assuming a narrow cone-beam angle. Traditionally, the contributions of the central rays are accumulated to construct the slice sensitivity profile at the isocenter of the scanner gantry. The slice sensitivity profile has been widely used to depict the slice thickness. However, the slice thickness depends on the interpolation algorithm that is used to synthesize complete planar data sets for the transaxial sections under reconstruction. It may be argued that the goodness of the pitch in spiral CT should be solely determined by the scanning/sampling pattern, that is, should be a feature inherent to the sampled data. In other words, the spiral scanning pattern specifies the longitudinal sampling pattern of the direct and opposite central rays, and the arrangement of sample loci dictates the sensitivity in any subsequent data interpolation from these samples, just as what was formulated in the preceding subsection.

Figure 1 defines the multislice spiral CT scanning and imaging geometry. As shown in Fig. 1(a), the three key parameters in multislice spiral CT are the longitudinal dimension of the detector collimation D, the number of detector arrays N, and the table increment per source rotation T, where the unit can be either mm or cm. The spiral scanning pitch p is directly related to the detector collimation and the table increment, defined as their ratio, $p=T/D$. Because of the narrow-angle cone-beam configuration (the cone angle relative to the midplane is less than 0.4°; see p. 555 in Ref. 6), the central rays of fan beams are assumed as parallel in this study, as illustrated in Fig. 1(b). Physically, multiple detector rows in the multislice spiral CT are arranged as shown in Fig. 1(a). Hence, the ideal longitudinal sampling is generally impossible where the central rays of the fan beams intersect a common transverse plane with equiangular intervals around the longitudinal axis. Therefore, the image quality does not decrease monotonically as the pitch increases.

Figure 2 shows sampling patterns of direct and opposite central rays from a single helical turn as well as multiple helical turns, respectively. The single turn case is important, because it is the basic element of an elongated helical scan, and may be increasingly useful in clinical applications as the cone-beam angle becomes larger. In the single turn case, the

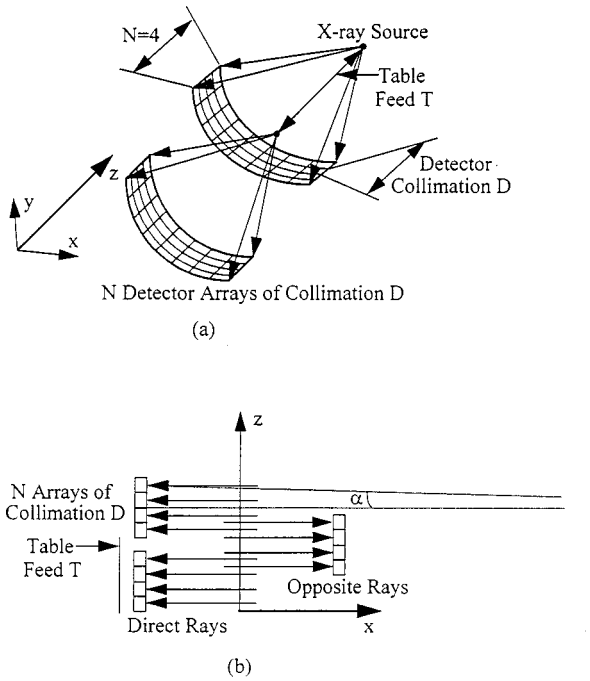

FIG. 1. Multislice spiral/helical CT geometry with the three key parameters: the detector collimation D, the number of detector arrays N, and the table increment per source rotation T. (a) 3D illustration of narrow-angle cone-beams, (b) direct and opposite central rays that are approximately parallel, since the narrow cone angle α is typically less than 0.4°.

total number of longitudinal samples is simply $L=2N$ for a given x-ray source orientation, as shown in Fig. 2(a). On the other hand, in the multiple turn case, the total number of longitudinal samples over a given longitudinal range depends on the pitch, and approximately is inversely proportional to the pitch, as shown in Fig. 2(b). Note that pitch is in turn dependent on the table feed (T) and detector dimension (D). Equivalently, the analysis on the effect of pitch could be presented in terms of a fixed T or D as the other parameter is varied. Formulas for the exact sampling locations can be geometrically derived in either of the cases,[8] but are not included here for brevity.

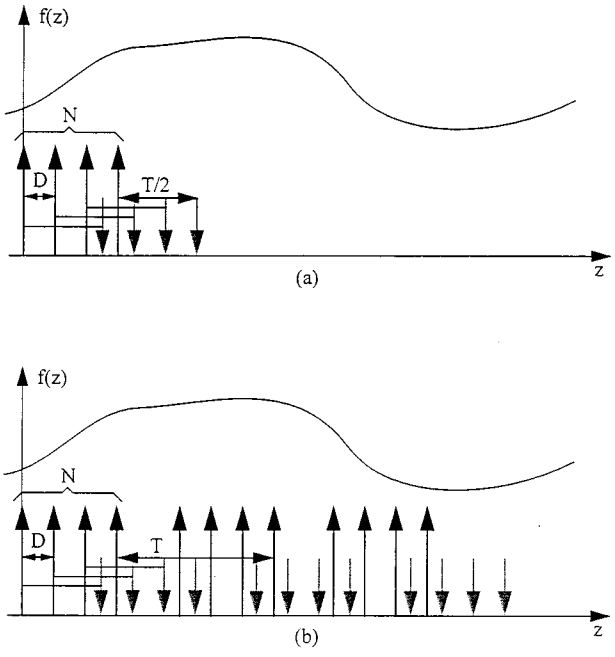

FIG. 2. Sampling patterns of direct and opposite central rays from (a) a single scanning turn, and (b) multiple scanning turns, where D denotes the detector collimation, N the number of detector arrays, and T the table increment per source rotation.

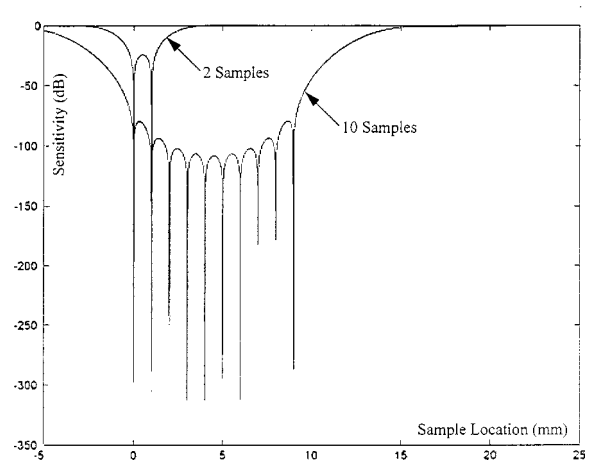

FIG. 3. Sensitivity of signal reconstruction over the range of $[-5, 25]$ in mm from 2 and 10 uniformly sampled locations shown as the minimum points (adapted from Fig. 1 in Ref. 12, using values computed by our MATLAB program).

III. NUMERICAL ANALYSIS

To demonstrate the utility of the sensitivity analysis approach in the study on the effect of pitch in multislice spiral CT, numerical simulation was done based on representative parameters of the current multislice spiral CT scanners. Specifically, four detector arrays were used, the detector collimation D was set to 2 mm, and the data longitudinal bandwidth was selected to be consistent with the detector collimation, that is, Δ in Eq. (1) was set to 2 mm. Our software for the sensitivity analysis of the effect of pitch in multislice spiral CT was coded in the MATLAB language (MathWorks, Inc., Natick, MA), and run on a personal computer Gateway 2000 P5-120 (120 MHz Pentium, 32 MB RAM; Gateway 2000, Inc., North Sioux City, SD).

Figure 3 shows the sensitivity of signal reconstruction from a uniformly sampled data set consisting of two and ten samples. As expected, the sensitivity at the sampling positions is the lowest; it increases when the reconstruction position is away from the sampling positions, and the more the samples, the lower the sensitivity. The results in Fig. 3 not only help visualize the idea of the sensitivity analysis, but also serve to verify the correctness of our software, since they are in excellent agreement with those reported in Ref. 16. The y-axis scale for sensitivity is given in terms of decibels, which indicates the large dynamic range for this parameter, requiring a special care in computation (double floating data). The cause for different sensitivity values at the sampling locations is the finite precision of computation.

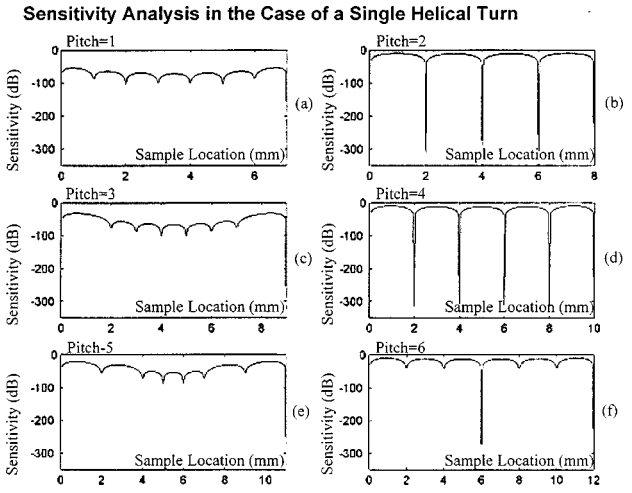

FIG. 4. Sensitivity of multislice spiral CT sampling from a single helical turn, where the detector collimation $D=2$ mm, the number of detector arrays $N=4$, and the pitch $p=1,2,...,6$ for (a)–(f), respectively. Note that the interval of the abscissa is defined by the minimum and maximum sampling locations, hence they vary from plot to plot.

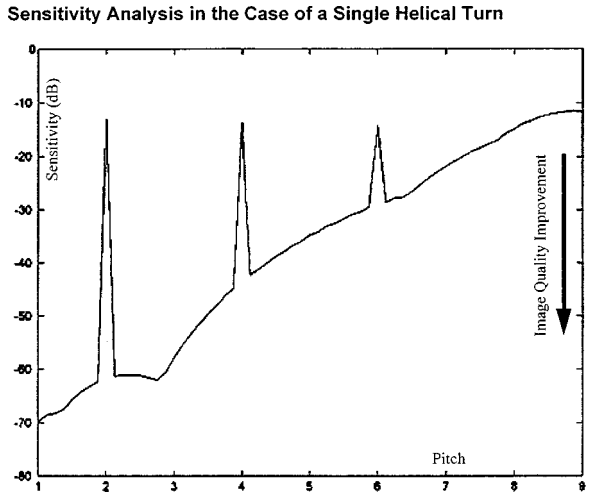

FIG. 5. Median sensitivity of multislice spiral CT sampling as a function of the pitch, computed under the same conditions as for Fig. 4, where the detector collimation $D=2$ mm, the number of detector arrays $N=4$, and the pitch interal is [1,9].

Theoretically, the sensitivity value at any sampling location must be 0 (minus infinite in dB). We strongly underscore the fact that higher values of sensitivity under this definition give less performance (that is, worse image quality).

Although the sensitivity function is most informative for any specific pitch in multislice spiral CT, a figure of merit is desirable to describe the overall quality of the sampling pattern associated with that pitch, and subsequently to optimize the scanning protocol relative to the pitch. Clearly, this figure of merit should reflect the global sensitivity in a heuristic manner. In this study, each sensitivity curve was visually examined for the overall deviation from the 0 dB line, and quantitatively represented by the median value of the sensitivity function.[22] The median value was chosen for its appropriateness in capturing our visual impression on the distance between the sensitivity curve and the 0 dB line. As compared to the mean value, the median value is less sensitive to outliers and errors in computing the sensitivity. Note that fluctuation in the sensitivity, as measured in dB, is great around the sampling locations, and this randomness can be effectively suppressed via median filtering. Also, note that the minimum of the sensitivity function should be always achieved at sampling locations.

Figure 4 includes six sensitivity plots of multislice spiral CT sampling from *a single helical turn* for the pitches of 1,2,...,...,...,6, respectively. Figure 5 is the corresponding sensitivity-pitch plot, which is the median sensitivity curve of multislice spiral CT sampling as a function of the pitch from 1 through 9 with a step length of 0.1, computed under the same conditions as in Fig. 4. In the single turn case, the sensitivity functions were computed in the interval defined by the two extreme central rays. Figures 6 and 7 show our results in the case of *multiple helical turns*, which are the counterparts of Figs. 4 and 5. In the multiple turn case, the sensitivity functions were computed in (0,20), which is spanned by the direct and opposite rays from one helical turn with the maximum pitch ($p=9$).

Figure 4 shows that the overall sensitivity decreases in general as the pitch increases. Quite high sensitivity is associated with pitches of 2, 4, and 6. In these high pitch cases, superposition occurs with both direct and opposite rays. The median sensitivity curve in Fig. 5 reconfirms this phenomenon with peaks at pitches of 2, 4, and 6. This sensitivity-pitch curve also shows that a pitch of a little less than 3 is preferred that gives volume coverage larger than pitch 2 and interpolation sensitivity less than pitches 2 and those greater than 3. Similar comments can be made on Figs. 6 and 7. Note that the ''harmonic oscillation'' pitches (at which direct and opposite central rays of the fan beams overlap to various extents) should be avoided, because these pitchs, such as pitches of 2, 4, and 6, lead to peaks of the sensitivity-pitch curve.

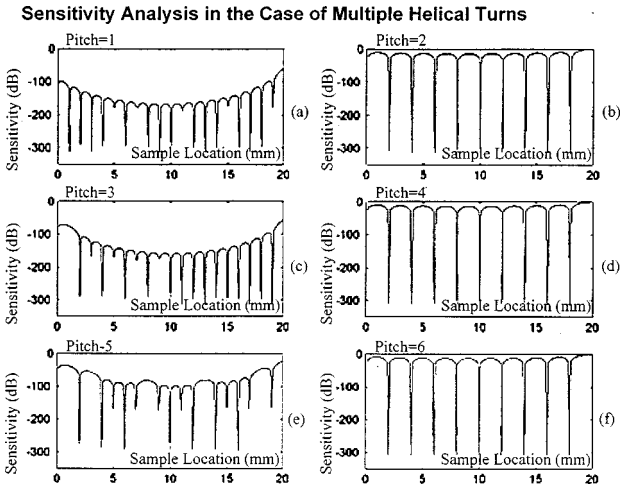

FIG. 6. Sensitivity of multislice spiral CT sampling from multiple helical turns, where the detector collimation $D=2$ mm, the number of detector arrays $N=4$, and the pitch $p=1,2,...,6$ for (a)–(f), respectively.

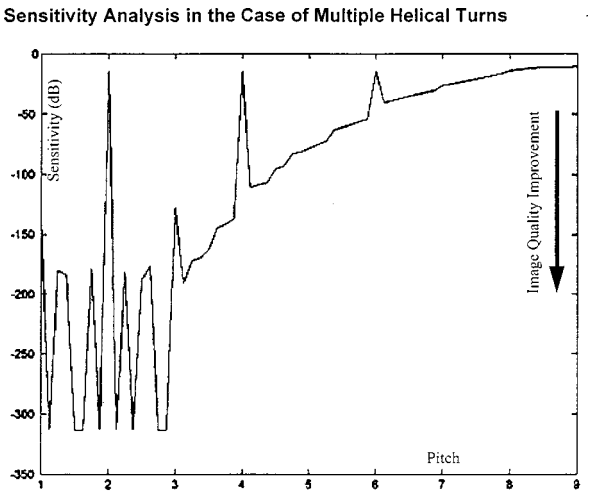

FIG. 7. Median sensitivity of multislice spiral CT sampling as a function of the pitch, computed under the same conditions as for Fig. 6, where the detector collimation $D=2$ mm, the number of detector arrays $N=4$, and the pitch interval is [1,9].

It is recognized that our results indicate a pitch of 6 to be a local maximum for sensitivity (i.e., decreased image quality), whereas at least one vendor uses that pitch as a point of optimal image quality.[8] This discrepancy may be explained as follows. The sampling pattern does not uniquely determine the method for image reconstruction, although it dictates image quality in a fundamental way. In other words, some other factors, such as the interpolation algorithm, might be playing a relevant role. However, as far as the sensitivity of multislice spiral CT data interpolation is concerned, a pitch of 6 is not a good choice.

IV. DISCUSSIONS AND CONCLUSION

We have demonstrated that a pitch study in multislice spiral CT can be performed based on the sampling pattern in the Radon domain, and the specifics of the algorithms for raw data interpolation do not play any explicit role. This methodology is advantageous in at least two aspects. First, the sensitivity function, directly derived from the sampling pattern, is quite fundamental regarding the potential and limitation of data interpolation in multislice spiral CT. Second, the effect of pitch can be examined using the sensitivity analysis approach without involvement of either testing objects or raw data interpolation, which may lead to higher efficiency in scanner design and protocol optimization. Actually, raw data interpolation details are often considered proprietary by manufacturers of CT scanners, and are currently unavailable to us.

Although our work reported in this paper was restricted to the central rays of the fan beams, the methodology can be applied to study the sensitivity of interpolation from data associated with all available x-rays. This extension would provide a complete picture of sensitivity of raw data interpolation in multislice spiral CT. and would be a reasonable indicator of image reconstruction quality. If the temporal dimension is added in the sensitivity analysis, the system performance can be described in both spatial and temporal terms. Clearly, the computational requirements for more sophisticated sensitivity studies would be very high, especially for singular value decomposition, which is needed to determine the null space of the sampling system.

The sensitivity of spiral CT data interpolation is directly related to the longitudinal bandwidth of signal. It is intuitively clear that given a sampling pattern, the wider the signal bandwidth, the less susceptible the signal reconstruction. Because the emphasis of this paper is comparison among different sampling patterns associated with various pitches, the relationship between the sensitivity and the bandwidth is not quantified in this study. However, this topic deserves further research.

The predictive value of the sensitivity of multislice spiral sampling needs experimental evaluation and validation using well-known indexes, especially those for image resolution and image noise. Image artifacts are also an important aspect of image quality. Although these tasks have not been systematically performed yet, our findings are consistent with published knowledge on four-slice spiral CT.[1,2,6] In one study, a scanning method was developed for superior longitudinal sampling density by adding fractions and shifting data trials slightly. For example, it was found that the pitch of 2.5 is quite satisfactory,[6] image quality is higher when (1) the pitch is 3.5 than it is 3, and (2) the pitch is 4.5 than it is 4.[2] In another study, it was pointed out that unlike single-slice spiral CT, multislice spiral CT has favored pitches, suggesting the pitch of 3 is better than the pitch of 2.[1] It is emphasized that the slice sensitivity profile should not be supplanted by the sensitivity analysis. The value of this particular analysis lies in determination of the underlying ''goodness'' of the sampled data set.

When wide-angle cone-beam spiral CT scanners emerge in the future, the fan-beams defined by individual detector arrays will no longer be in parallel, but our sensitivity analysis approach can still be applied to quantify the effect of pitch. One way for the sensitivity analysis of helical scanning in this wide cone-beam angle case is to work in the Feldkamp-type reconstruction framework. The Feldkamp algorithm[23] has been the most popular practical cone-beam algorithm, but it is limited by circular scanning and longitudinal image blurring. The Feldkamp cone-beam algorithm was generalized to allow flexible scanning loci for microtomography.[7,24] The generalized Feldkamp cone-beam algorithm can be adapted in special cases, such as helical scanning.[7,24] Recently, the generalized Feldkamp algorithm was reformulated in two steps: (1) cone-beam to fan-beam data conversion via a cosine correction, and (2) fan-beam reconstruction via filtered backprojection.[25] As a result, after wide-angle cone-beam data associated with direct and opposite x-rays are weighted by appropriate cosine factors, they can still be regarded as from fan-beams that are in parallel to the gantry plane. Hence, the sensitivity of data interpolation in the wide cone-beam angle case can be similarly analyzed.

In conclusion, using the recently developed sensitivity analysis approach,[16] we modeled the effect of pitch on raw data interpolation in multislice spiral CT. Our results reveal

the characteristic sensitivity of multislice spiral sampling for recovery of Radon data, facilitating understanding of relationships among pitch, data interpolation sensitivity, and image reconstruction quality in multislice spiral CT, and may be valuable for design of multislice spiral CT scanners and imaging protocol optimization in clinical applications.

ACKNOWLEDGMENTS

The authors thank anonymous reviewers for the constructive comments. This work was supported in part by grants from the National Institutes of Health, Grant Nos. DC03590, DK50184, and NS35368.

[a]Electronic mail: ge-wang@uiowa.edu

[1] S. H. Fox, L. N. Tanenbaum, S. Ackelsberg, H. D. He, J. Hsieh, and H. Hu, ''Future directions in CT technology,'' in *Neuroimaging Clinics of North America*, edited by L. L. Berland (W. B. Saunders, Philadelphia, 1998), pp. 497–513.

[2] Y. Saito, ''Multislice x-ray CT scanner,'' Toshiba Med. Rev. **98**, 1–8 (1998).

[3] S. Schaller, ''Spiral reconstruction for a multirow detector CT system,'' Radiology **205**, 214 (1997).

[4] T. Flohr, ''Clinical benefits of a multirow detector spiral CT system,'' Radiology **205**, 214–215 (1997).

[5] K. Taguchi and H. Aradate, ''A new algorithm and evaluation for image reconstruction in multislice helical CT,'' Radiology **205**, 390 (1997).

[6] K. Taguchi and H. Aradate, ''Algorithm for image reconstruction in multislice helical CT,'' Med. Phys. **25**, 550–561 (1998).

[7] G. Wang, T. H. Lin, P. C. Cheng, and D. M. Shinozaki, ''A general cone-beam reconstruction algorithm,'' IEEE Trans. Med. Imaging **12**, 486–496 (1993).

[8] H. Hu, ''Multislice helical CT: scan and reconstruction,'' Med. Phys. **26**, 5–18 (1999).

[9] D. V. Paranjpe and C. J. Bergin, ''Spiral CT of the lungs: Optimal technique and resolution compared with conventional CT,'' Am. J. Roentgenol. **162**, 561–567 (1994).

[10] G. D. Rubin and S. Napel, ''Increased scan pitch for vascular and thoracic spiral CT,'' Radiology **197**, 316–317 (1995).

[11] M. Funke, L. Kopka, U. Fischer, J. W. Oestmann, and E. H. Grabbe, ''Spiral CT of pulmonary nodules: Comparison of 2:1 and 1:1 pitch,'' Radiology **193**, 339 (1994).

[12] S. Blake, T. Toma, F. L. Flanagan, and E. Breatnach, ''Comparison of thoracic helical CT protocols performed at 1:1 pitch and 2:1 pitch,'' Radiology **193**, 339 (1994).

[13] C. E. Woodhouse and J. L. Friedman, ''*In vitro* air-contrast-enhanced spiral 3D CT (virtual colonoscopy) appearance of colonic lesions,'' Radiology **197**, 500 (1995).

[14] G. Wang and M. W. Vannier, ''Maximum volume coverage in spiral CT,'' Acad. Radiol. **3**, 423–428 (1996).

[15] G. Wang and M. W. Vannier, ''Optimal pitch in spiral computed tomography,'' Med. Phys. **24**, 1635–1639 (1997).

[16] A. Tarczynski, ''Sensitivity of signal reconstruction,'' IEEE Signal Process. Lett. **4**, 192–194 (1997).

[17] G. Wang and M. W. Vannier, ''Longitudinal resolution in volumetric x-ray CT—Analytical comparison between conventional and helical CT,'' Med. Phys. **21(3)**, 429–433 (1994).

[18] B. W. Jones, *Linear Algebra* (Holden-Day, San Francisco, 1973).

[19] G. Wang and W. Han, ''Minimum error bound of signal reconstruction,'' IEEE Signal Process. Lett. (in press).

[20] C. R. Crawford and K. F. King, ''Computed tomography scanning with simultaneous patient translation,'' Med. Phys. **17**, 967–982 (1990).

[21] A. Polacin, W. A. Kalender, and G. Marchal, ''Evaluation of section sensitivity profiles and image noise in spiral CT,'' Radiology **185**, 29–35 (1992).

[22] W. H. Press, S. A. Teukolsky, W. T. Vetterling, and B. P. Flannery, *Numerical Recipes in C—The Art of Scientific Computing*, 2nd ed. (Cambridge University Press, Cambridge, 1992).

[23] L. A. Feldkamp, L. C. Davis, and J. W. Kress, ''Practical cone-beam algorithm,'' J. Opt. Soc. Am. A **1**, 612–619 (1984).

[24] G. Wang, T. H. Lin, P. C. Cheng, D. M. Shinozaki, and H. Kim, ''Scanning cone-beam reconstruction algorithms for x-ray microtomography,'' SPIE Proc. **1556**, 99–113 (1991).

[25] G. Wang, S. Y. Zhao, and P. C. Cheng, ''Exact and approximate cone-beam x-ray microtomography,'' in *Modern Microscopies*, edited by P. C. Cheng, P. P. Huang, J. L. Wu, G. Wang, and H. G. Kim (Springer-Verlag, New York, in press), Vol. 1.